Journal of Oceanology and Limnology
Vol. 38 No. 1, P. 42-54, 2020
https://doi.org/10.1007/s00343-019-8298-3

Impact of emulsification of crude oil on normalized radar cross section*

GUO Jie[1, 2, 3, **], ZHANG Tianlong[1, 4], ZHANG Xi[5, **], LIU Genwang[5]

[1] *CAS Key Laboratory of Coastal Environmental Processes and Ecological Remediation*, *Yantai Institute of Coastal Zone Research* (*YIC*), *Chinese Academy of Sciences* (*CAS*) , *Yantai 264003*, *China*

[2] *Shandong Key Laboratory of Coastal Environmental Processes*, *YICCAS*, *Yantai 264003*, *China*

[3] *Center for Ocean Mega-Science*, *CAS*, *Qingdao 266071*, *China*

[4] *University of Chinese Academy of Sciences*, *Beijing 100049*, *China*

[5] *First Institute of Oceanography* (*FIO*), *Ministry of Natural Resources* (*MNR*), *Qingdao 266061*, *China*

Received Oct. 23, 2018; accepted in principle Feb. 1, 2019; accepted for publication Mar. 25, 2019

Abstract The emulsification of crude oil is caused by the oil flowing into the water, resulting in the increase of oil film tension, viscosity, water content, and volume, which brings great harm to the marine ecological environment and difficulties for the cleanup of marine emergency equipment. The realization observation of emulsification crude oil will increase the response speed of marine emergency response. Therefore, we set up crude oil emulsification samples to study the physical property in laboratory and conducted radar measurements at different incidence angles in outdoor. The radar is C band in resolution of 0.7 m by 0.7 m. A fully polarimetric scatterometer (HH, VV, and VH/HV) is mounted at 1.66 m (minimum altitude) height at an incidence angle between 35° and 60°. An asphalt content of less than 3% crude oil and the filtered seawater were used to the outdoor emulsification scattering experiment. The measurement results are as follows. The water content can be used to describe the process of emulsification and it is easy to measure. Wind speed, asphalt content, seawater temperature, and photo-oxidation affect the emulsifying process of crude oil, and affects the normalized radar cross section (NRCS) of oil film but wind is not the dominant factor. It is the first time to find that the emulsification of crude oil results in an increase of NRCS.

Keyword: emulsification of crude oil; normalized radar cross section (NRCS); water content; wind speed; temperature

1 INTRODUCTION

Emulsification occurs when crude oil enters the sea and produces a water-in-oil (W/O) emulsion (Thingstad and Pengerud, 1983). A large amount of water is adsorbed by the crude oil, which affects its tension, viscosity, and volume (Fingas, 1995; Fingas and Fieldhouse, 1999; Yan and Xu, 2002; Khan et al., 2011). Emulsification makes it difficult to remove crude oil from seawater after oil spills, and prevents effective operation of most mechanical recovery equipment. The increase of the viscosity of emulsified crude oil can easily suffocate marine animals, and the toxic substances in the marine environment are more harmful to the marine environment. The use of remote sensing to monitor crude oil emulsification in real time would be beneficial for implementation of oil spill responses and to reduce the associated risks.

For crude oil emulsions, the importance of a rigid and protective film surrounding the water droplets is usually pointed out (Johansen et al., 1988). Asphalt, colloids, and wax in crude oil play different roles in the emulsification process (Mackay and Zagorski, 1982; Berridge et al., 1986; Sjoblom et al., 1990). A W/O emulsion is formed when water droplets are dispersed throughout a continuous oil phase (Fig.1) (Khan et al., 2011; Wong et al., 2015). Neuman and

* Supported by the National Natural Science Foundation of China (No. 41576032) and the Major Program for the International Cooperation of the Chinese Academy of Sciences, China (No. 133337KYSB20160002); partially supported by the National Natural Science Foundation of China (Nos. 41576170, 61371189)
** Corresponding authors: jguo@yic.ac.cn; xi.zhang@fio.org.cn

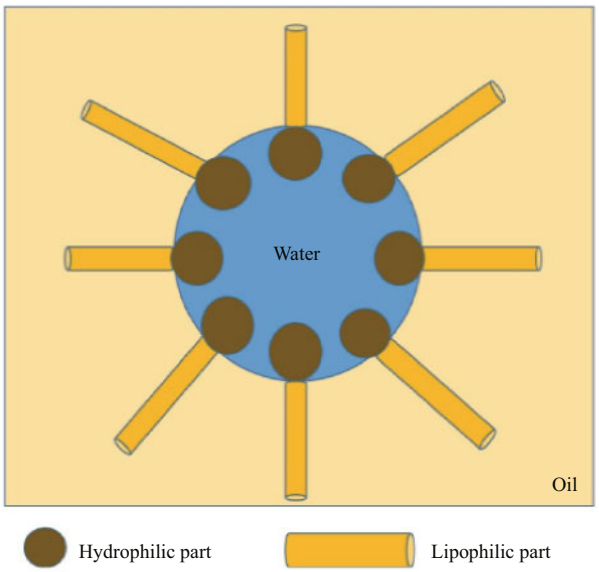

Fig.1 An illustration of a water-in-crude oil emulsion

Paczyńska-Lahme (1988) thought that oil itself was a microemulsifier in the oil phase of asphalt and colloids, and that the emulsion was stabilized by a surfactant, with the large hydrophobic part and the small hydrophilic part of the surfactant beneficial to formation of a hydroemulsion. Bora (1991) found that emulsion formation was the result of undissolved polar substances and asphaltenes behaving in a similar manner to surfactants in oil. However, asphaltenes are easily dissolved by volatile aromatic compounds in oil, and only form an emulsion when the content of volatile aromatic demulsification material decreases to <3% through evaporation and there is inadequate bitumen or gelatin (>3%) to form an emulsion. Colloid has a certain stabilizing effect, but it is worse than asphalt (Daling and Brandvik, 1988; Fingas, 1995). Evaporation removes light components and enhances the emulsification process through its effect on the asphaltene concentration. Photooxidation forms new surfactants to promote the emulsification process (Thingstad and Pengerud, 1983). Light and physical mixing play essential roles in the formation of water-in-oil emulsions (Thingstad and Pengerud, 1983).

The influence of temperature on emulsification can vary. High temperature is beneficial to oil and water mixing, and can accelerate formation of emulsification. Based on observations of the color, viscosity, elasticity, zero shear rate of viscosity, moisture content, and electrical conductivity, Fingas et al. (Fingas, 1995; Fingas and Fieldhouse, 1999) defined emulsions as stable (asphalt content >7%), semi-stable (3% < asphalt content <7%), and unstable (asphalt content <3%). The temperature, shear rate, and water volume fraction greatly affect the viscosity of a W/O (Ariffin et al., 2016). Emulsification can increase the volume of an oil spill by two to five times of the original volume, the density from the original density of around 0.80 g/mL increase to a maximum of 1.03 g/mL, and the viscosity from a few hundred millipascal seconds to one hundred thousand millipascal seconds. This will produce a heavy and semi-solid material (Fingas, 1995; Fingas and Fieldhouse, 2003, 2004; Yue et al., 2017).

Many domestic and international studies have investigated oil spill detection using scattering experiments. Theses experiment can be performed indoors or outdoors. In 1971, THN (The Hague, Netherlands) established an observation station on the coast of Norway based on a non-phase-coherent pulse system using infrared sensors and an airborne side-view radar to measure sea surface wind waves and oil spillage. In addition, NIWARS (Netherlands Interdepartmental Working Community on the Application of Remote Sensing) built an indoor wind and wave sink (100 m long, 8 m wide, and 0.5 m high), which was used to simulate the effect of wind on the water surface (De Loor and Van Hulten et al., 1998; Li, 2014; Guo et al., 2016). In 1992, the Institute of Oceanography at the University of Hamburg (Germany) placed light and heavy fuel oil samples along the North Sea coast. Spilled oil measurements were conducted in four bands (X, C, S, and L) with a scattering meter and the differences between experimental measurements of water samples from the oil spill area and theoretical values were evaluated. In laboratory, a number of studies have been carried out in a small (26-m long, 1-m wide, 0.5-m depth) wind-wave flume (Li, 2014; Guo et al., 2016). Offshore oil spill measurements has been carried out with light diesel oil (4 300 kg) on the surface of the sea west of Xiachuan Island (Hainan, China) by the South China Sea Institute of Oceanology of the Chinese Academy of Sciences. Using an aircraft as a platform, an 8-mm microwave radiometer was used to measure the brightness temperature of the oil on the sea surface (Yang et al., 1998). Four bands (L, S, C, and X) were used for measurements in a semi-microwave darkroom at the University of Electronic Science and Technology of China, Chengdu in 2007. Two antennas were placed adjacent to each other, and HH, VV, HV, and VH polarization scattering measurements were carried out. The effects of

different wavelengths, types of polarization, wind speeds and directions, and oil film thickness on the sea surface scattering coefficient were evaluated (Li, 2014). Wu (1986) showed that the surface roughness of the oil film was affected more than the direction function of the scattering field.

SAR plays an increasingly important role due to little interference from rain and cloud in the observation of oil spill at sea surface. A detailed introduction to oil spill detection by satellite remote sensing is given by Brekke and Solberg (2005), while a detailed comparison on the several approaches and their characteristics is given by Topouzelis (2008). The change of normalized radar cross section (NRCS) was oil spills appear as dark areas in the SAR images, because the oil dampens the capillary waves of the sea surface caused by the change of oil film roughness (Fingas and Brown, 1997; Solberg et al., 2007; Solberg et al., 2007; Karantzalos and Argialas, 2008; Liu et al., 2010). Traditional methods of oil film recognition use several semi-automatic and automatic detection algorithms based on neural networks, for which multi-scale image segmentation and fuzzy logic have been developed to detect oil slicks in single-polarization (Del Frate et al., 2000; Solberg et al., 2007; Garcia-Pineda et al., 2009; Liu et al., 2010). With the development of full-polarization satellites, polarimetric SAR decomposition parameters, average alpha angle, and entropy were estimated for oil-slick contaminated sea surfaces and slick-free conditions using a RADARSAT-2 quad-polarization SAR image (Zhang et al., 2011). The focus of the researchers has been to remove a look-alike phenomenon, such as currents, eddies, upwelling or downwelling zones, fronts and rain cells, etc. Multiple methods of remote sensing to distinguish between different types of oil spill are also being tried.

The effect on the NRCS of emulsification of crude oil has not been investigated. The oil spill emulsification process increases the moisture content and changes the surface roughness of the oil film, which should affect the NRCS. At present, there is no clear text to describe the degree of emulsification of crude oil. However, it is generally accepted that 'chocolate mousse' or the crude oil turned brown occurs completely emulsified (Fingas, 1995; Fingas and Fieldhouse, 2003, 2004; Wong et al., 2015). In this paper, we try to describe the emulsification process with moisture content, and the variation of crude oil emulsification highlights NRCS changes to be observed by scatterometer in outdoor.

2 MATERIAL AND METHOD

2.1 Material

The asphalt content, density, moisture content, wax content, and colloid content of the dehydrated crude oil were 1.35%, 0.93 g/cm^3, 0.64%, 11.07%, and 28.76%, respectively. The emulsion of this crude oil was unstable. Filtered seawater was used in all experiments. An auxiliary study on emulsified moisture content of crude oil was with an asphalt content of more than 7%.

A trace water meter (SCKF105), automatic tension tester (SCZL203), rotational viscometer (NDJ-8S), multi-function circulating constant temperature water bath (HWY-10), 40× microscope, and electric mixer (JJ-2A) were used in the laboratory experiments.

A crude oil of the asphalt content 1.35% emulsification experiment was conducted in an outdoor fiberglass pool (6-m long, 2.2-m wide, and 0.7-m depth). The pool had filtered seawater and seawater density was 1.02 g/mL, which was injected at a depth of 0.35 m, the mass of seawater was 4 700 kg.

A C-band microwave scatterometer (VV, HH, VH and HV polarization; 0.75 m resolution, the radar noise floor is about from -50 dB to -40 dB) was used to observe the NRCS during the crude oil emulsification process. A small weather station was located about 200 m from the pool. A UV fluorescence tester was to measure the volatilization of polyaromatic hydrocarbons. SCKF105 was to measure the moisture content of the crude oil emulsion.

2.2 Method

2.2.1 The characteristics of emulsified crude oil observation with different moisture content

The formula for calculating moisture content is as follows:

$$W_c=100\%\times W_m/(O_m+W_m), \quad (1)$$

where W_c is moisture content and W_m is the weight of water; O_m is the weight of oil.

At room temperature (25°C), crude oil (200 g) was placed in a 2-L beaker with Wm of seawater by calculation from formula 1. The solution was mixed (600 r/min) for 20 min by JJ-2A, and then the beaker was sealed and left for 24 h. Afterwards, we observed whether there was water at the bottom of the beaker. If there was no water at the bottom of the beaker, according to the Eq.1, the amount of water needed for different moisture content is calculated. More

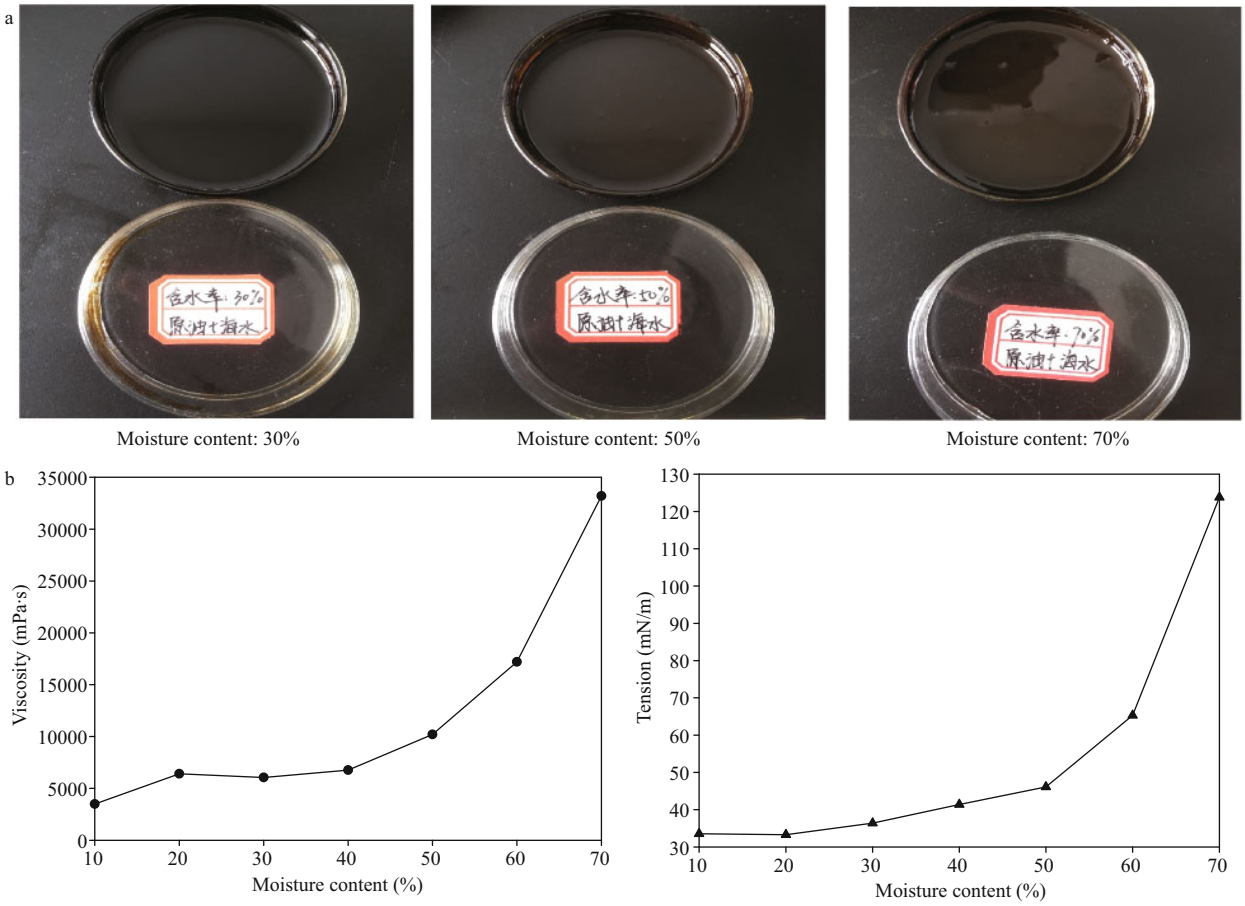

Fig.2 The different moisture content 30%, 50% and 70% emulsion crude oil (a) relationship between viscosity, tension and moisture content (b) from asphalt content of more than 7%

seawater was added based on the observed moisture content, and the above procedure was repeated. This process was continued until there was some water at the bottom of the beaker at the end of the 24 h. The different moisture content 30%, 50%, and 70% from asphalt content of more than 7% emulsion crude oil in Fig.2a. The color changed from black to brown (chocolate mousse) after the crude oil was completely emulsified from moisture content more than 50%. From Fig.2b, the tension (measured by SCZL203) and viscosity (measured by NDJ-8S) are positively correlated with the moisture content, especially when the moisture content is 50% and the tension and viscosity are obviously increased. When the moisture content is 70% fully saturated, the tension is 4 times, and the viscosity is 9 times comparing with the moisture content 10%.

Although unstable emulsified crude oil does not appear brown. However, it is relatively beneficial to the study of the effect of crude oil emulsification with moisture content. Therefore, we describe the process of emulsification of crude oil with moisture content in this

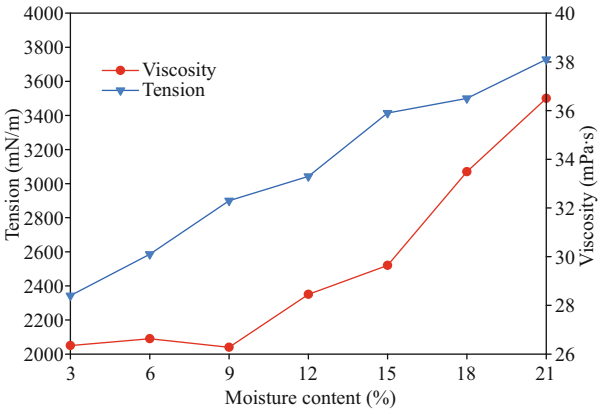

Fig.3 The relationship between the oil emulsification tension, viscosity, and moisture content at 25°C from asphalt content of less than 3%

paper. The volume of water added was used to calculate the maximum moisture content of the oil at 25°C. In the emulsification process of the asphalt content 1.35%, the tension and viscosity increased as the moisture content increased, but the viscosity and tension were no more than one order of magnitude greater than that of the starting oil (Fig.3). It is an unstable emulsion.

Table 1 The influence of different factors in the crude oil emulsion scattering experiment

Numerical code	Mass (g)	Temperature (°C)	Hand stirring (+) One night (*)	Wind speed (m/s)	Moisture content (%)
1 (water)	4 700 000	23.4		1.32	
2 (oil) (2017/8/23/17:21)	1	32.1		4.67	
3 (2017/8/24/10:03)	1	30	*	6.58	
4 (2017/8/24/10:20)	62	30		5.86	
5 (2017/8/23/11:02)	62	30.9	+(2 min)	6.04	
6 (2017/8/23/17:21)	62	30.9		6.13	
7 (2017/8/24/16:03)	62	34	+(2 min)	4.94	
8 (2017/8/24/16:36)	135.7	34.2	+(2 min)	5.95	
9 (2017/8/24/17:56)	135.7	33	+	5.25	
10 (2017/8/25/8:02)	135.7	28	*	2.21	
11 (2017/8/25/8:58)	225.7	28	+(2 min)	5.38	
12 (2017/8/25/10:30)	225.7	29		5.94	
13 (2017/8/25/13:35)	225.7	31		5.82	
14 (2017/8/25/15:48)	445.7	33	+(2 min)	4.43	
15 (2017/8/25/16:57)	445.7	33		5.10	
16 (2017/8/26/8:10)	445.7	28.5	*	2.81	
17 (2017/8/26/10:06)	3 821.7	33		2.43	6
18 (2017/8/26/11:12)	3 821.7	31	+(3 min)	2.66	14.7
19 (2017/8/26/13:48)	3 821.7	33	+(5 min)	2.48	7.4
20 (2017/8/26/16:33)	3 821.7	32	+(10 min)	3.29	34.6
21 (2017/8/27/7:50)	3 821.7	28	*	1.10	21.9
22 (2017/8/27/10:09)	4 841.7	30	+(10 min)	1.74	30.2
23 (2017/8/27/10:50)	4 841.7	31.5	+(10 min)	1.22	5.8
24 (2017/8/27/14:26)	5 896.7	32	+(10 min)	2.41	9.1
25 (2017/8/27/15:00)	5 896.7	32	+(10 min)	2.33	57
26 (2017/8/27/16:22)	6 996.7	31	+(10 min)	2.75	45
27 (2017/8/27/17:30)	6 996.7	31	+(10 min)	3.57	42.9

The plus symbol indicates 2–10 min of stirring, and the asterisk indicates the solution was left over night with no oil adding or stirring. The number 1 is sea water and the numbers from 2–27 are crude oil.

Therefore, relatively stable emulsions of different moisture contents can be formed in different temperature ranges. The stable maximum saturation moisture content of relatively stable emulsions was 21% at 25°C and 12% at 20°C. In the emulsification process, the tension and viscosity were directly proportional to the moisture content. The experiment found that relatively stable moisture content could reflect emulsification process of unstable emulsions.

A small sample (asphalt content <3%) of different moisture content (0.64%, 6%, and 12%) were applied to the glass slide and placed under 40× magnification (Fig.4). A higher degree of emulsification resulted in more water droplets in the emulsion of crude oil and the water droplet diameter was less than 0.3 mm. The moisture content can be used to describe the process of emulsification of crude oil and is easy to measure by SCKF105 (Yue et al., 2017).

2.2.2 Outdoor crude oil emulsion scattering experiment

Observations were performed from Aug. 23 to 27 2017 at the Muping Coastal Environment Research Station of the Chinese Academy of Sciences. Observation by the scatterometer was recorded and the addition of crude oil within 0.5 h time interval was observed and recorded. Wind speed (V) and air temperature data from weather station are averaged over 0.5 h. The oil temperature was recorded using a thermometer. Oil was added to the pool nine times in 5 days, and the cumulative crude oil mass was 6 996.7 g (Table 1). Because of instrument limitations, the UV fluorescence tester was used after the first and second additions of crude oil only. A schematic diagram of the experiment is shown in Fig.5. A fully polarimetric scatterometer (HH, VV, and VH/HV) is mounted at 1.66 m (minimum altitude) height at an incidence angle

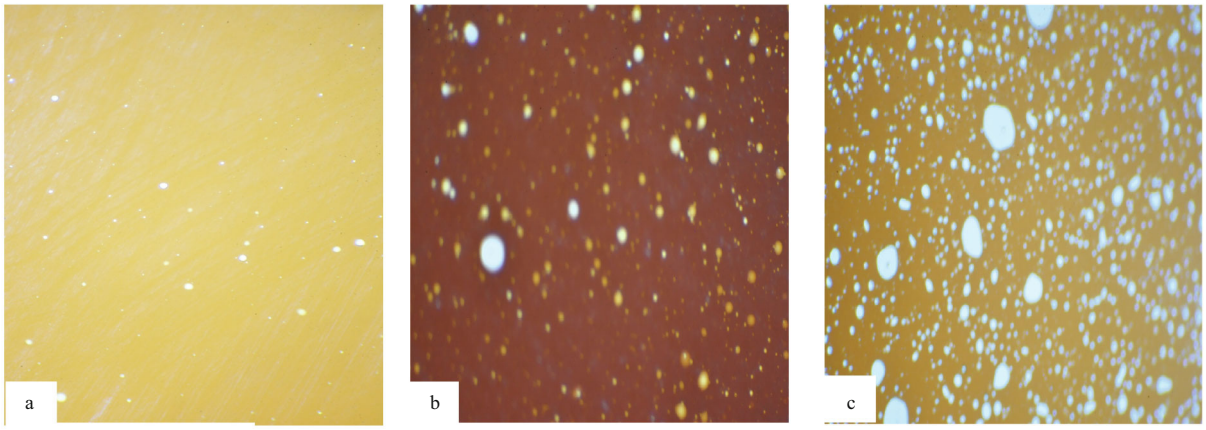

Moisture content: 0.64% Moisture content: 6% Moisture content: 12%

Fig.4 Images of the moisture content in emulsions at 20°C under a 40-fold microscope

The white points are water droplets. a. crude oil 0.64% moisture content; b. 6% moisture content; c. 12% moisture content.

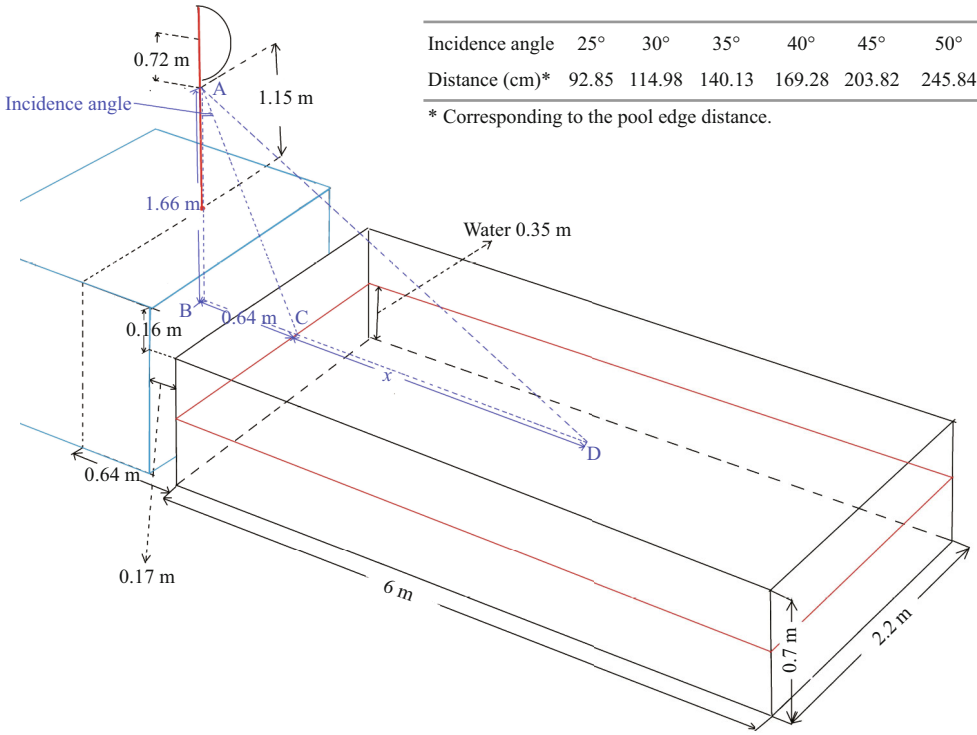

Incidence angle	25°	30°	35°	40°	45°	50°	55°	60°
Distance (cm)*	92.85	114.98	140.13	169.28	203.82	245.84	298.60	367.52

* Corresponding to the pool edge distance.

Fig.5 Experimental set up

x (CD) represents the horizontal distance of the different incident angles in the side of pool (see Distance).

between 25° and 60°. The distance between the scatterometer and the surface of the water at each angle of incidence is shown in the table in Fig.5.

Scatterometer observations of the surface of the water in the pool show that angles of incidence from 35° to 60° are suitable (Fig.6). Due to the limitation of the pool, the wave height caused by the wind is only millimeters, so it was ignored. The NRCS of seawater and the NRCS of 1-g oil film decreased as the angle of incidence increased (Fig.6a, b). The NRCS with HH polarization was unusually low when the angle of incidence was 40° for local reasons. The NRCS values with VV and HV polarization were similar with angles of incidence of greater than 45°. When the angle of incidence was greater than 40°, the NRCS with HH polarization was greater than that with the other types of polarization. Changes in the NRCS with 1 g of crude oil were very similar to those with just water (Fig.6a, b). The differences between the NRCS values of seawater (V was 5.07 m/s) and 1 g of crude oil (V was 4.67 m/s) at various angles of incidence are shown in Fig.6c, and temperatures of seawater and oil are 31.9°C and 32.1°C, respectively. With HH polarization at angles of incidence of 40° and 45°, VV polarization at angles of

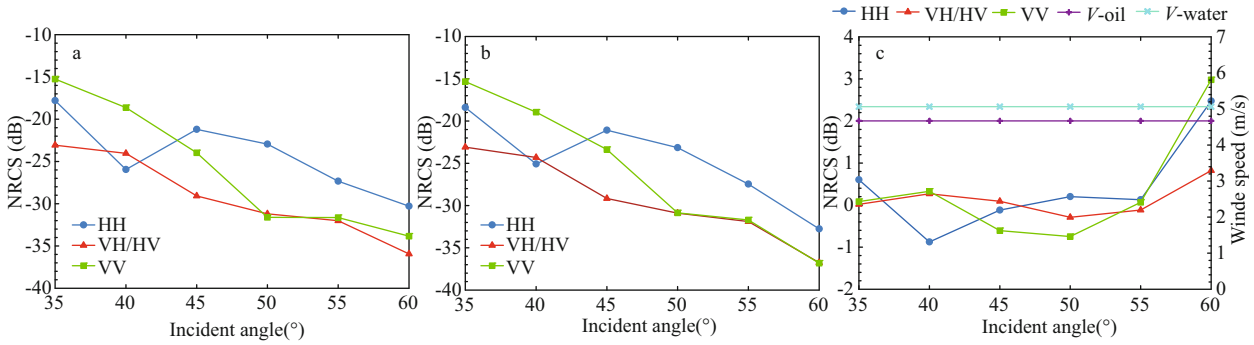

Fig.6 The NRCS of water (a) and an oil film formed with 1-g oil (b), and the difference between the NRCS of water and 1-g crude oil (c) at angles of incidence from 35° to 60° (measurement points 2 in Table 1)

V-water: wind speed on the surface of the water; *V*-oil: wind speed on the surface of the crude oil.

incidence of 45° and 50°, VH/HV polarization at angles of incidence of 50° and 55°, and a *V* of 4.67 m/s on the oil film, the NRCS values were higher than those of seawater with a *V* of 5.07 m/s. It is well known that the oil film dampens the surface capillary gravity wave and causes NRCS to decrease. However, as shown in Fig.6c, conclusion is opposite from such a result. Statistical difference between the NRCS values of seawater and crude oil emulsion in different polarization modes at different incidence angles shows that the difference more than zero was accounted for 70.5% (HH), 37.8% (VV), and 30.8% (VH/HV), respectively (Fig.7). Due to various reasons, the NRCS of VV and VH/HV polarization are relatively close when the incidence angle is greater than 45° in this experiment. By comparing the above-mentioned differences, it can be seen that the proportions of NRCS more than zero from VV and VH/HV are relatively close, but the proportion of NRCS from HH is very high. There was only one reason for this result: the emulsification of crude oil led to increase NRCS. Figure 7 shows that the differences between the NRCS values of seawater and crude oil emulsified are more than zero, with the crude oil mass distribution between 135.5 g and 445.7 g in No. 8–16 of Table 1 and the NRCS maximum increment value in the location of the incident angles are greater than 45°. Due to the uneven spread of crude oil on the seawater surface and the uncertainties of factors such as wind, the emulsification of the experimental oil was also uneven for causing this phenomenon.

Among the angles of incidence, 45° provided the best observations of the influence of crude oil emulsification on the NRCS values for all three types of polarizations (HH, VV, and VH/HV). The factors influencing crude oil emulsification in the outdoor scattering experiment are shown in Table 1. The numbers 2 to 27 are the serial number of the observation crude oil emulsion. Figure 8 shows NRCS of crude oil emulsion at 45° incidence angle. Measurement point 1 in Fig.8a is for the NRCS of seawater, and measurement points 2 to 27 are for the NRCS of crude oil emulsification. The UV fluorescence tester showed that the aromatic hydrocarbons were almost completely evaporated in less than 30 min when in the crude oil was emulsified (measurement points 2–7, Fig.8a). For all three types of polarization, the NRCS of crude oil increased as the wind speed decreased (measurement point 2 compared to 1 point (water), Fig.8a) and the similar phenomena are repeated in Fig.8a. This shows that the oil film NRCS changed by emulsification of the crude oil. This change was more obvious with HH polarization, followed by VV polarization, and then VH/HV polarization. The crude oil used in the experiments was unstable. The moisture content of the crude oil stabilized overnight when the pool was covered with canvas, and the NRCS values with the three types of polarization all decreased at same time in a wind speed of 6.58 m/s at point 3. The NRCS values of the three types of polarization gradually increased from measurement point 4 to 6 (Fig.8a). Then, the NRCS decreased at measurement point 7 after addition of 62 g of crude oil (Fig.8a). The change in the NRCS with VH/HV polarization was less obvious than the changes with the other types of polarization. To accelerate the emulsification process, we used stirring from measurement point 5 to 27 (Table 1, Fig.8a). Points 3, 10, 16, and 21 show where the emulsified crude oil was left over night. It was found that the NRCS had a remarkable rise or fall during the night. This indicates that the photooxidation, wind speed, and temperature had an effect on the emulsification of crude oil. The results are consistent largely with the trend of rising or falling and show a relative stable state in moisture content of the crude oil emulsion. From measurement points 7 to 9, 14 to

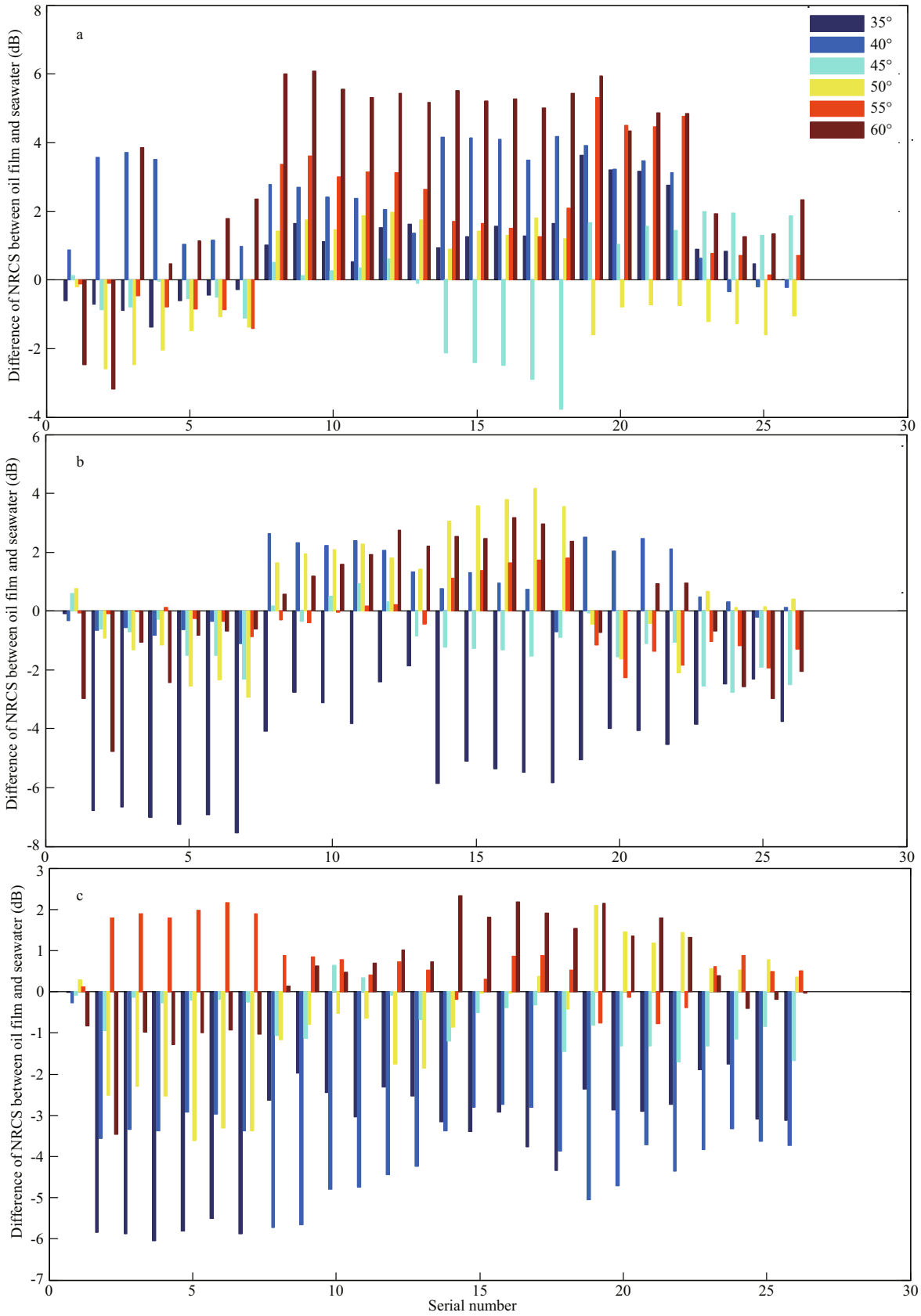

Fig.7 The difference between NRCS value of crude oil and seawater emulsified distribution at angles of incidence from 35° to 60° (data from Table 1)

a. HH; b. VV; c. VH/HV.

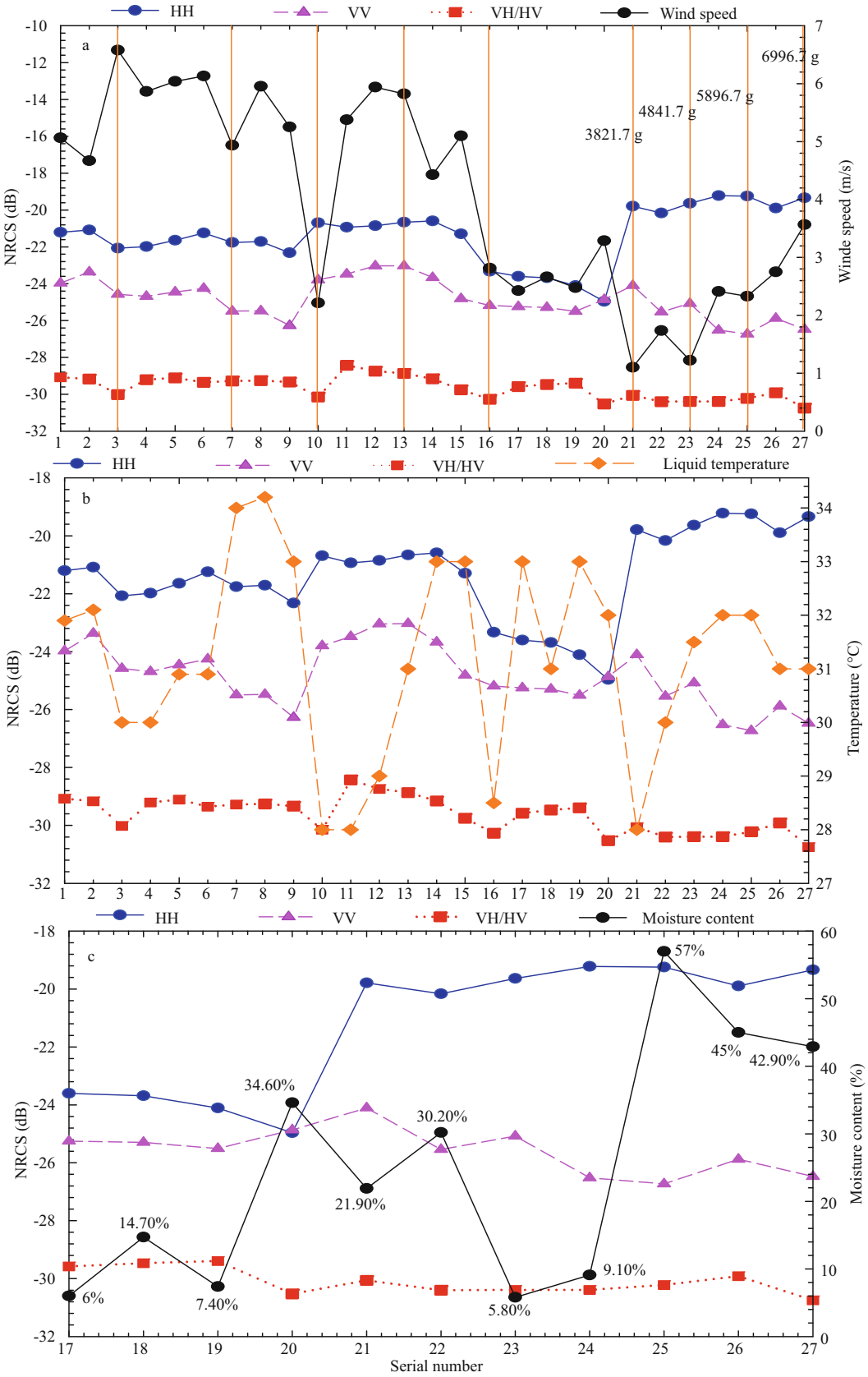

Fig.8 Changes in the NRCS during the emulsification process of crude oil with HH, VH/HV, and VV polarization in different wind speed at 45° incidence angle

a. with different wind speed; b. with different liquid temperature; c. with different moisture content.

15, and 17 to 19 (exclusive of 18) at over 33°C, the NRCS obtained with HH, VV, and VH/HV polarization were decreasing (Fig.8b). The cumulative crude oil to 445.7 g was easy to emulsify thin oil film. The maximum amplitude of HH, VV, and VH/HV were 3.01, 3.2, and 1.75 dB from 1 to 16 (Fig.8a). From measurement point 17 to 27, accumulative oil was 6 996.7 g. The maximum amplitude of HH, VV, and VH/HV were 5.74, 2.70, and 1.39 dB in Fig.8a and the NRCS with all three types of polarization disagree in the thick oil film in which the NRCS of HH changed greatly, and the VV and VH/HV were relatively small compared with the thin oil film. These differences were caused by the increased oil volume, the short duration of emulsification, and inhomogeneity. Observation of moisture content was limited by oil film thickness, and we measured the moisture content in oil at 3 821.7 g (at serial number 17 in Table 1). From measurement point 17 to 27 (Table 1) high moisture content did not correspond to high oil temperature, and fluctuations in the moisture content accompanied the emulsification and demulsification processes because of the low asphalt content of the crude oil. The moisture content of crude oil at 28°C was relatively stable at 22% (Table 1). Therefore, the corresponding NRCS increased when the moisture content was 21.9% (Fig.8c). Figure 8 shows that the wind speed is not positively correlated with NRCS. The range of NRCS at HH, VV, and VH/HV varied from -19.22 to -24.95 dB, from 23.04 to -26.73 dB, and from -28.43 to -30.78 dB at 45°, respectively.

3 DISCUSSION

The moisture content of the relatively stable crude oil emulsions at oil temperatures of 20 and 25°C were 12% and 21%, respectively (Section 2.2.1). At an oil temperature of 28°C, the moisture content of the relatively stable crude oil emulsion was 22% (Section 2.2.2). Because the asphalt content of the crude oil was less than 3%, it is an unstable emulsion. These results show that the moisture content of a relatively stable emulsion, in which no demulsification occurred within a week under static conditions, is affected by the temperature. For a relatively stable emulsion, the tension is positively correlated with the viscosity.

Outdoor conditions are very beneficial to the emulsification process because of rapid evaporation and the influence of V and light oxidation. Figure 9 shows that the NRCS of crude oil emulsions changed at different incidence angles from HH, VV, and VH/HV; and the NRCS decreases as the incidence the angle increases (except 40°). The range of NRCS at HH, VV, and VH/HV varied from -14.15 to -33.48 dB, from -15.24 to -38.62 dB, and from -23.07 to -39.41 dB, respectively, and the NRCS of crude oil emulsions was not positively correlated with wind speed at different angles of incidence in three polarized ways. When incident angle is greater than the 45°, the NRCS of crude oil emulsion in VV and VH values are similar, which is consistent with the observed NRCS of seawater (Fig.6a, b). We think that the NRCS decreases gradually with the increase of incident angle, the NRCS of VV and VH values of crude oil emulsion are close to each other due to noise.

It is well known that the NRCS decreases because oil films dampen propagation of capillary gravity wave. The only explanation for this abnormal result is that emulsification of crude oil changes the scattering mechanism of the oil film surface, leading to an increase in the NRCS. The wind speed is not the main cause of the variation of oil film NRCS (Fig.9). Field test photos are shown in Fig.10.

4 CONCLUSION

Crude oil, with an asphalt content of less than 3%, can be emulsified in seawater under ambient conditions. The relative saturation moisture content of the unstable emulsion influenced by temperature, but the emulsification was not optimized at high temperatures (over 33°). Stirring will speed up the emulsification or demulsification for unstable emulsified crude oil. Wind speed is not positively correlated with NRCS of emulsification crude oil film observations. A certain degree of emulsification can increase the NRCS and the maximum increment is 6.08 dB at HH, 4.15 dB at VV, and 2.34 dB at HV in this experiment, and the maximum root-mean-square error compared with seawater was 4.38, 5.25, and 4.19 dB, respectively at HH, VV, and VH. In NRCS observations of a thin or a thick oil film, HH polarization is the best, followed by VV polarization, and then VH/HV polarization.

The increase of NRCS is affected by the degree of emulsification. Because oil emulsification changes the structure of oil film, the scattering of oil film is changed. However, we found that the higher the degree of emulsification, the smaller the NRCS. It is speculated that the NRCS of emulsified oil film with a certain thickness can be increased. This requires further experiments.

The emulsification and demulsification processes

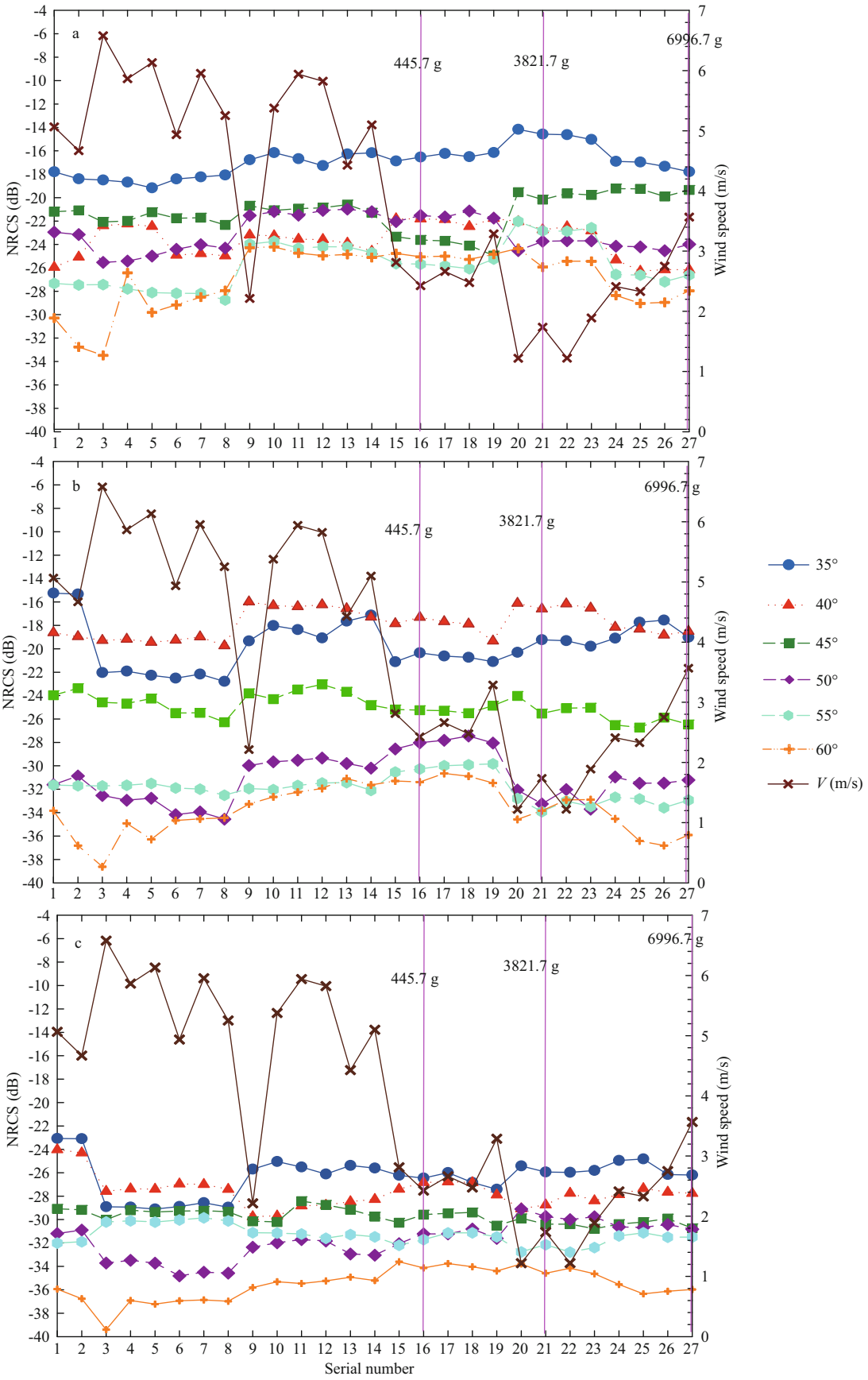

Fig.9 The NRCS of crude oil emulsions changed at different incidence angle and *V* HH (a); VV (b); VH/HV (c)

Fig.10 Photos of oil spill test site

of crude oil change the NRCS of the crude oil film. We did not quantify description the contributions of wind speed and the moisture content of emulsification to the NRCS due to sewage treatment. In future studies, we will use crude oil with an asphalt content of >7% to study the emulsification characteristics, and the relationship between emulsifying moisture content, dielectric constant, and NRCS was established. Because transmission of electromagnetic waves in the medium is inevitable, there will be anti-radiation, scattering, and transmission phenomena. In the process of emulsification, microwave passes through the air and oil to the water, and then to the oil and into the water. Electromagnetic scattering can occur on a rough surface of the multilayered medium. The influence of the emulsification on the NRCS will be described quantitatively and the scattering mechanism will be studied in subsequent experiments; and the detail associated remote sensing mechanism of the emulsification crude oil will be done elsewhere.

5 DATA AVAILABILITY STATEMENT

Data are available on request from the authors.

6 ACKNOWLEDGMENT

We thank Muping Coastal Environment Research Station of the Chinese Academy of Sciences for field support and for using the weather station observation data.

References

Ariffin T S T, Yahya E, Husin H. 2016. The rheology of light crude oil and water-in-oil-emulsion. *Procedia Engineering*, **148**: 1 149-1 155.

Berridge S A, Dean R A, Fallows R G, Fish A. 1986. The properties of persistent oils at sea. *Journal of the Institute of Petroleum*, **54**: 300-309.

Bora M A. 1991. Water-in-oil emulsification: a physicochemical study. *In*: International Oil Spill Conference.American Petroleum Institute, Washington, DC. p.483-488.

Brekke C, Solberg A. 2005. Oil spill detection by satellite

remote sensing. *Remote sensing of Environment*, **95**(1): 1-13.

Daling S, Brandvik J. 1988. A study of the formation and stability of water-in-oil emulsions. *In*: Proceedings of the 11th Arctic Marine Oilspill Program Technical Seminar. Environment Canada, Ottawa. p.153-170.

De Loor G P, Van Hulten H W B. 1998. Microwave measurements over the North Sea. *Boundary-Layer Meteorology*, **13**(1-4): 119-131.

Del Frate F, Petrocchi A, Lichtenegger J, Calabresi G. 2000. Neural networks for oil spill detection using ERS-SAR data. *IEEE Transactions on Geoscience and Remote Sensing*, **38**(5): 2 282-2 287, https://doi.org/10.1109/36.868885.

Fingas M F, Brown C E. 1997. Review of oil spill remote sensing. *Spill Science & Technology Bulletin*, **4**(4): 199-208.

Fingas M F, Fieldhouse B. 1999. Water-in-oil emulsions results of formation studies and applicability to oil spill modelling. *Spill Science & Technology Bulletin*, **5**(1): 81-91.

Fingas M, Fieldhouse B. 2003. Studies of the formation process of water-in-oil emulsions. *Marine Pollution Bulletin*, **47**(9-12): 369-396, https://doi.org/10.1016/S0025-326X(03)00212-1.

Fingas M, Fieldhouse B. 2004. Formation of water-in-oil emulsions and application to oil spill modelling. *Journal of Hazardous Materials*, **107**(1-2): 37-50, https://doi.org/10.1016/j.jhazmat.2003.11.008.

Fingas M. 1995. Water-in-oil emulsion formation: a review of physics and mathematical modelling. *Spill Science & Technology Bulletin*, **2**(1): 55-59, https://doi.org/10.1016/1353-2561(95)94483-Z.

Garcia-Pineda O, Zimmer B, Howard M, Pichel W, Li X F, MacDonald I R. 2009. Using SAR images to delineate ocean oil slicks with a texture-classifying neural network algorithm (TCNNA). *Canadian Journal of Remote Sensing*, **35**(5): 411-421.

Guo J, Meng J M, He Y J. 2016. Scattering model research based on two-dimensional laser observation of spilled oil and emulsification processes. *Marine Sciences*, **40**(2): 159-164. (in Chinese with English abstract)

Johansen E J, Skjärvö M, Lund T, Sjöblom J, Söderlund H, Boström G. 1988. Water-in-crude oil emulsions from the Norwegian continental shelf Part I. Formation, characterization and stability correlations. *Colloids and Surfaces*, **34**(4): 353-370.

Karantzalos K, Argialas D. 2008. Automatic detection and tracking of oil spills in SAR imagery with level set segmentation. *International Journal of Remote Sensing*, **29**(21): 6 281-6 296, https://doi.org/10.1080/01431160802175488.

Khan B A, Akhtar N, Khan H M S, Waseem K, Mahmood T, Rasul A, Iqbal M, Khan H. 2011. Basics of pharmaceutical emulsions: a review. *African Journal of Pharmacy and Pharmacology*, **5**(25): 2 715-2 725, http://doi.org/10.5897/AJPP11.698.

Li Y. 2014. Research on Microwave Scattering Properties of Oil Spill Based on Experimental method. University of Electronic Science and Technology of China, Chengdu. p.1-85. (in Chinese with English abstract)

Liu P, Zhao C F, Li X F, He M X, Pichel W. 2010. Identification of ocean oil spills in SAR imagery based on fuzzy logic algorithm. *International Journal of Remote Sensing*, **31**(17-18): 4 819-4 833, https://doi.org/10.1080/01431161.2010.485147.

Mackay D, Zagorski W. 1982. Water-in-oil emulsions: a stability hypothesis. *In*: Proceedings of the Fifth Annual Arctic Marine Oilspill Program Technical Seminar. Environment Canada, Ottawa. p.61-74.

Neuman H J, Paczyńska-Lahme B. 1988. Petroleum emulsions, micro-emulsions, and micellar solutions. *In*: Hummel K, Schurz J eds. Dispersed Systems. Steinkopff Verlag, Darmstadt. p.123-126.

Sjoblom J, Urdahl O, Borve K G N. 1990. Stabilization and destabilization of water-in-oil emulsions from the Norwegian continental shelf: correlation with model systems. *Advances in Colloids and Polymer Science*, **41**(1992): 241-271.

Solberg A H S, Brekke C, Husoy P O. 2007. Oil spill detection in radarsat and envisat SAR images. *IEEE Transactions on Geoscience and Remote Sensing*, **45**(3): 746-755.

Thingstad T, Pengerud B. 1983. The formation of 'chocolate mousse' from Stafjord crude off and seawater. *Marine Pollution Bulletin*, **14**(6): 214-216.

Topouzelis K N. 2008. Oil Spill Detection by SAR images: dark formation detection, feature extraction and classification algorithms. *Sensors*, **8**(10): 6 642-6 659.

Wong S F, Lim J S, Dol S S. 2015. Crude oil emulsion: A review on formation, classification and stability of water-in-oil emulsions. *Journal of Petroleum Science and Engineering*, **135**: 498-504.

Wu J. 1986. Research on microwave backscattering of sea-surface with oil slick. *Chinese Journal of Radio Science*, **3**(1): 32-44. https://doi.org/10.13443/j.cjors. 1986.03.003. (in Chinese with English abstract)

Yan Z Y, Xu H L. 2002. Review of the studies on emulsification of spilled oil. *Environmental Protection in Transportation*, **23**(2): 1-6, 26. (in Chinese with English abstract)

Yang Y Z, Lu G X, Zhong Q Y, Huang Y L, Zhou Z Z. 1998. A study on measuring the thickness of oil film on the sea by airborne remote sensing. *Remote Sensing of Environment China*, **8**(3): 222-231. (in Chinese with English abstract)

Yue H S, Guo J, Mu Y K, Zhang T L. 2017. Detection of oil film roughness of 3D laser scanner. *Journal of Guangxi Academy of Sciences*, **33**(4): 298-302, https://doi.org/10.13657/j.cnki.gxkxyxb.20171127.002. (in Chinese with English abstract)

Zhang B, Perrie W, Li X F, Pichel W G. 2011. Mapping sea surface oil slicks using RADARSAT-2 quad-polarization SAR image. *Geophysical Research Letters*, **38**(10): L10602, https://doi.org/10.1029/2011GL047013.